

# **3-D resistivity inversion with electrodes displacements**

**M.H.Loke (Geotomosoft Solutions)**

**P. B. Wilkinson and J.E. Chambers  
(British Geological Survey)**

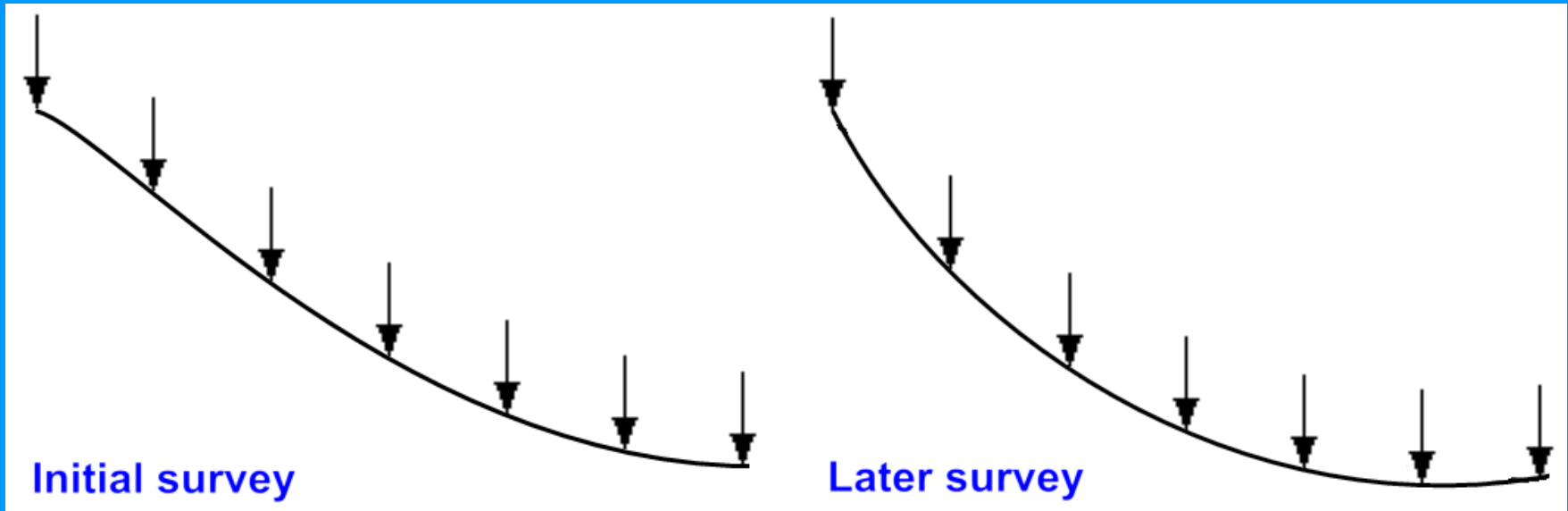
*Email : [geotomosoft@gmail.com](mailto:geotomosoft@gmail.com)*

# Outline

1. An outline of the problem
2. Least-squares inversion method and Jacobian matrix calculations
3. 3-D synthetic model and field survey examples
4. Conclusions

## Electrical surveys on unstable surfaces

Electrical surveys with repeated measurements are used to detect changes in the subsurface geology with time, possibly on unstable slopes. Positions of the electrodes are measured at the start and at intervals. Ground movements can occur between the times of the electrode positions measurements. Precise positions of the electrodes are not known and have to be estimated (together with the subsurface resistivity) from the resistivity data.



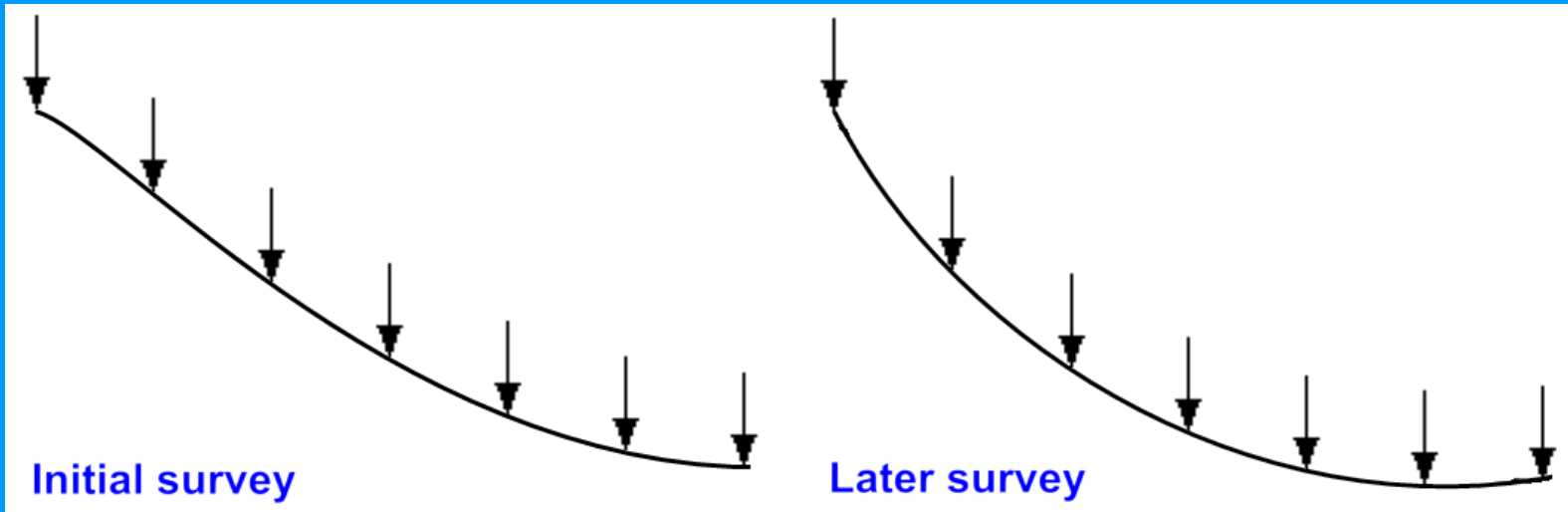
# The data inversion problem

What we have :-

- 1). Apparent resistivity data and positions of electrodes from initial survey.
- 2). Apparent resistivity data from later survey after electrodes movement.

What we want:-

True subsurface resistivity for both survey times, and positions of electrodes at later survey.



## The least-squares optimisation method

The smoothness-constrained least-squares method is commonly used in 2-D and 3-D resistivity inversion, using the following equation.

$$\left[ \mathbf{J}_i^T \mathbf{R}_d \mathbf{J}_i + \lambda_i \mathbf{W}^T \mathbf{R}_m \mathbf{W} \right] \Delta \mathbf{r}_i = \mathbf{J}_i^T \mathbf{R}_d \mathbf{g}_i - \lambda_i \mathbf{W}^T \mathbf{R}_m \mathbf{W} \mathbf{r}_{i-1}$$

$\mathbf{W}$  = roughness filter,  $\lambda$  = roughness filter damping factor

$\mathbf{r}_{i-1}$  = current inversion model,  $\Delta \mathbf{r}_i$  = change in model resistivity

$\mathbf{R}_m$ ,  $\mathbf{R}_d$  = model and data weighting matrices

$\mathbf{g}$  = data misfit,  $\mathbf{J}$  = Jacobian matrix of partial derivatives (change of apparent resistivity with model resistivity).

Starting from an initial model  $\mathbf{r}_0$ , we determine  $\Delta \mathbf{r}_i$  iteratively to refine the model  $\mathbf{r}_i$  until the data misfit  $\mathbf{g}$  is reduced to an acceptable level.

The model parameter vector  $\mathbf{r}$  contains the (logarithm) of the model resistivity values. It can be modified to include the electrodes positions.

## Modified least-squares optimisation method

The least-squares equation is modified to incorporate the (x,y,z) positions of the electrodes as model parameters.

$$\left[ \mathbf{G}_i^T \mathbf{R}_d \mathbf{G}_i + \lambda_i \mathbf{V}^T \mathbf{R}_m \mathbf{V} \right] \Delta \mathbf{q}_i = \mathbf{G}_i^T \mathbf{R}_d \mathbf{g}_i - \lambda_i \mathbf{V}^T \mathbf{R}_m \mathbf{V} \mathbf{q}_{i-1}$$

The model vector becomes  $\mathbf{q} = (r_1 \dots r_m, x_2 \dots x_e, y_2 \dots y_e, z_2 \dots z_e) = (\mathbf{r} \ \mathbf{x} \ \mathbf{y} \ \mathbf{z})$  if there are  $e$  electrodes and the first electrode is fixed.

The new Jacobian matrix becomes  $\mathbf{G} = (\mathbf{J} \ \mathbf{X} \ \mathbf{Y} \ \mathbf{Z})$

$\mathbf{X}$ ,  $\mathbf{Y}$  and  $\mathbf{Z}$  are the partial derivatives of the (logarithms) of the apparent resistivity values with respect to changes in the (x,y,z) positions of the electrodes.

The new roughness filter term becomes  $\mathbf{V} = (\mathbf{W} \ \alpha \mathbf{W}_x \ \beta \mathbf{W}_y \ \gamma \mathbf{W}_z)$

$\mathbf{W}_x$ ,  $\mathbf{W}_y$  and  $\mathbf{W}_z$  are the roughness filters for x, y and z with relative weights  $\alpha$ ,  $\beta$  and  $\gamma$ .

## Two issues with the modified least-squares method

The modified least-squares equation is

$$\left[ \mathbf{G}_i^T \mathbf{R}_d \mathbf{G}_i + \lambda_i \mathbf{V}^T \mathbf{R}_m \mathbf{V} \right] \Delta \mathbf{q}_i = \mathbf{G}_i^T \mathbf{R}_d \mathbf{g}_i - \lambda_i \mathbf{V}^T \mathbf{R}_m \mathbf{V} \mathbf{q}_{i-1}$$

**with**  $\mathbf{q} = (\mathbf{r} \ \mathbf{x} \ \mathbf{y} \ \mathbf{z})$ ,  $\mathbf{G} = (\mathbf{J} \ \mathbf{X} \ \mathbf{Y} \ \mathbf{Z})$  **and**  $\mathbf{V} = (\mathbf{W} \ \alpha \mathbf{W}_x \ \beta \mathbf{W}_y \ \gamma \mathbf{W}_z)$

There are 2 extra issues that needs to be resolved :-

- 1). Calculation of the spatial Jacobian matrices  $\mathbf{X}$  ,  $\mathbf{Y}$  and  $\mathbf{Z}$ .
- 2). Finding optimum values for the relative damping factors  $\alpha$ ,  $\beta$  and  $\gamma$ .

## Calculating the spatial Jacobian matrices

The terms in the  $\mathbf{X}$  spatial Jacobian matrix contains the change in the potential  $\Phi$  due to a change in the  $\mathbf{x}$  position of the electrode, such as

$$\frac{\partial \phi_i}{\partial x_2}$$

The potential values are calculated using the finite-element method by solving the matrix equation : -  $\mathbf{C}\Phi = \mathbf{s}$  .

$\mathbf{C}$  = capacitance matrix that depends on resistivity distribution and geometry of finite-element mesh

$\Phi$  = vector with the potentials at the nodes

$\mathbf{s}$  = vector with current sources at the nodes.

There are 2 main methods that are used to calculate the sensitivity values, the ‘perturbation’ and ‘adjoint-equation’ methods.



## Perturbation method – a brute force approach

The perturbation method calculates partial derivatives by re-solving the finite-element matrix equation  $\mathbf{C}\Phi = \mathbf{s}$  with a small change in the electrode position, such as

$$\frac{\partial \phi_i}{\partial x_2} \approx \frac{\phi_i(x_2 + \Delta x_2) - \phi_i(x_2)}{\Delta x_2}$$

The potentials only depend on the relative positions of the electrodes. We can fix the first electrode position. For a survey with 1001 electrodes, this method recalculates the potentials 3000 times for 3-D problems.

**Advantage :** Simple to implement in computer program.

**Disadvantage :** Very slow, impractical for 3-D. Possible directional bias. Not used for calculating resistivity Jacobian because it is too slow.

## Adjoint-equation method – a more elegant approach

A more efficient method is the adjoint-equation method that calculates the change in the potential  $\Phi$  from the change in the capacitance matrix  $\mathbf{C}$ . Differentiation of the capacitance matrix equation  $\mathbf{C}\Phi = \mathbf{s}$  wrt the  $x$ -position of an electrode gives

$$\mathbf{C} \frac{\partial \Phi}{\partial x_k} = - \frac{\partial \mathbf{C}}{\partial x_k} \Phi$$

It has the same form as the capacitance matrix equation. All the information needed to calculate  $\partial \Phi / \partial x_k$  is available in the process of solving  $\mathbf{C}\Phi = \mathbf{s}$  to calculate the potentials  $\Phi$ . It is not necessary to directly resolve the matrix equation.  $\partial \mathbf{C} / \partial x_k$  can be calculated using

$$\frac{\partial c_{pqr}}{\partial x_k} \approx \frac{c_{pqr}(\mathbf{x} + \Delta \mathbf{x}_k, y, z) - c_{pqr}(\mathbf{x} - \Delta \mathbf{x}_k, y, z)}{2 \Delta x_k}$$

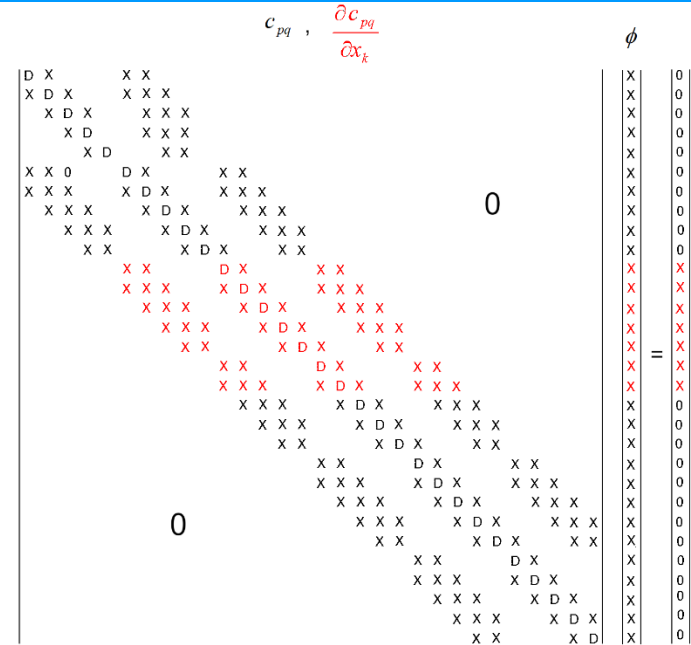
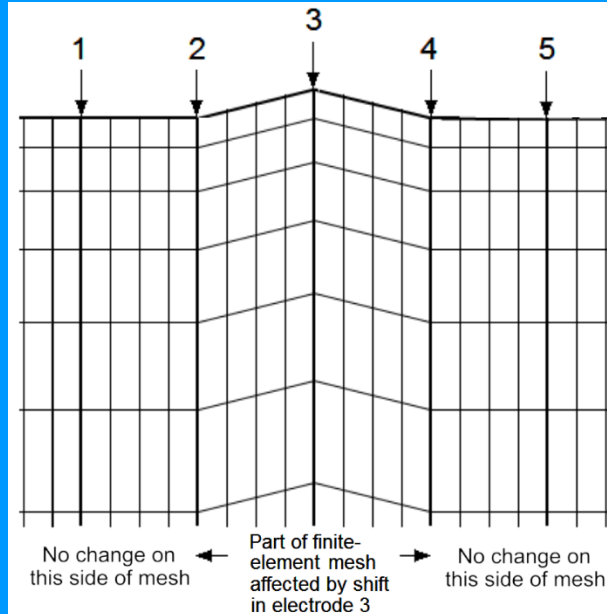
A two-sided difference is used to avoid directional bias. The time taken to calculate the  $c_{pqr}$  values is thousands of times less than resolving  $\mathbf{C}\Phi = \mathbf{s}$ .

## Further steps to reduce Jacobian matrix calculation time

We can also take advantage of (1) the very sparse nature of the **C** matrix, and (2) only a small number of matrix elements are affected by a shift at an electrode. In the 2-D example below, only nodes between electrodes 2 and 4 are affected by a shift in electrode 3. So only the  $\partial c_{pqr}/\partial x_k$  matrix elements associated with the affected nodes are non-zero.

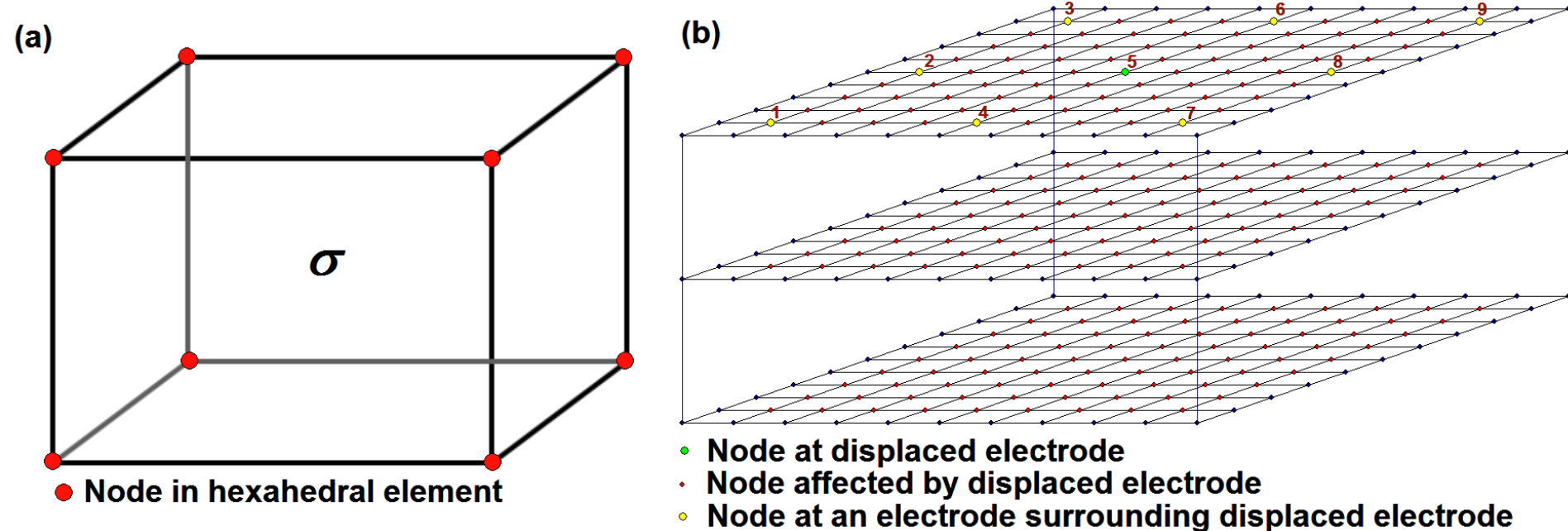
Calculation of the  $\partial\Phi/\partial x_k$  values only involves multiplication of a very sparse matrix with a vector.

In 2-D, the **C** matrix has only 9 non-zero diagonals.



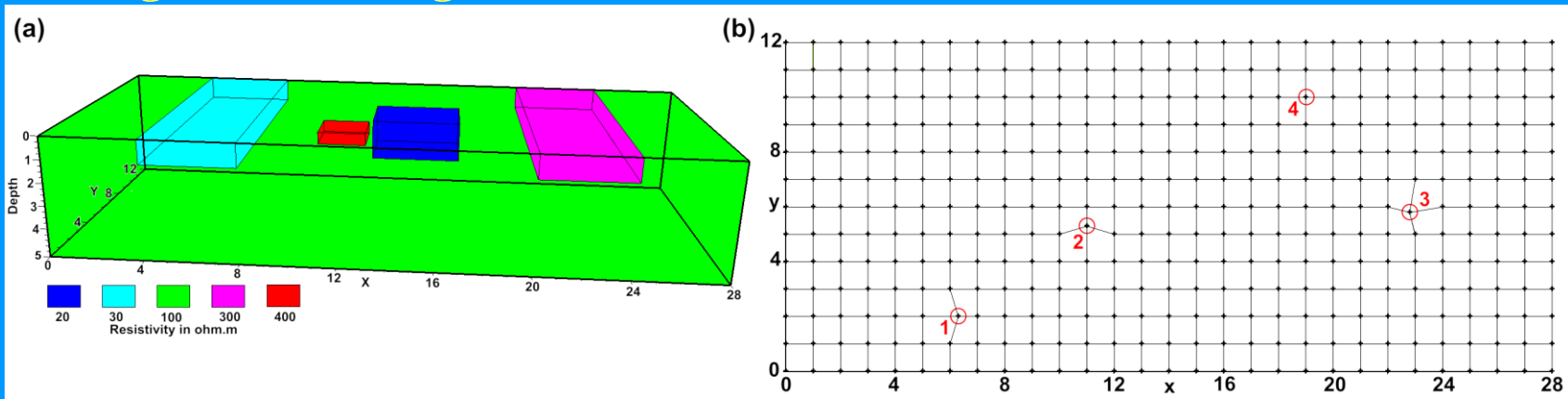
# 3-D mesh and spatial Jacobian matrix calculation

For 3-D problems, hexahedral finite elements are used. The **C** matrix has only 27 non-zero diagonals. A shift in an electrode position will only affect the mesh elements between it and 8 surrounding electrodes. Calculating the Jacobian matrix using the adjoint-equation method is thousands of times faster than the perturbation method.



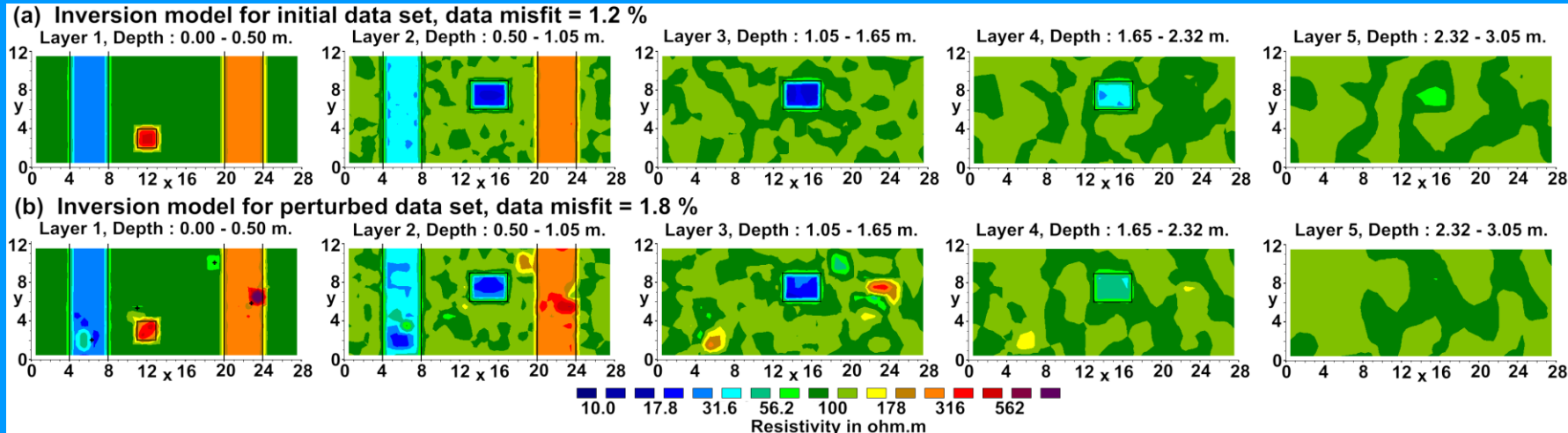
### 3-D test model setup

The model has a  $29 \times 13$  survey grid with electrode spacing of 1 m. It has a  $100 \Omega \cdot \text{m}$  background with two near surface bands of low ( $30 \Omega \cdot \text{m}$ ) and high ( $300 \Omega \cdot \text{m}$ ) resistivity. There is a shallow  $400 \Omega \cdot \text{m}$  prism and a deeper  $20 \Omega \cdot \text{m}$  resistivity prism. In the perturbed model, 3 electrodes (1,2,3) are shifted horizontally and 1 electrode (4) vertically, and the resistivities of the prisms are changed to 350 and  $25 \Omega \cdot \text{m}$ . The data set consists of 6573 dipole-dipole measurements along the  $x$  and  $y$  directions with a maximum geometric factor of 1056 m (i.e.  $a=1$  m and  $n=6$ ). Voltage dependent Gaussian noise was added to the data that gave an average noise level of 1.1%.



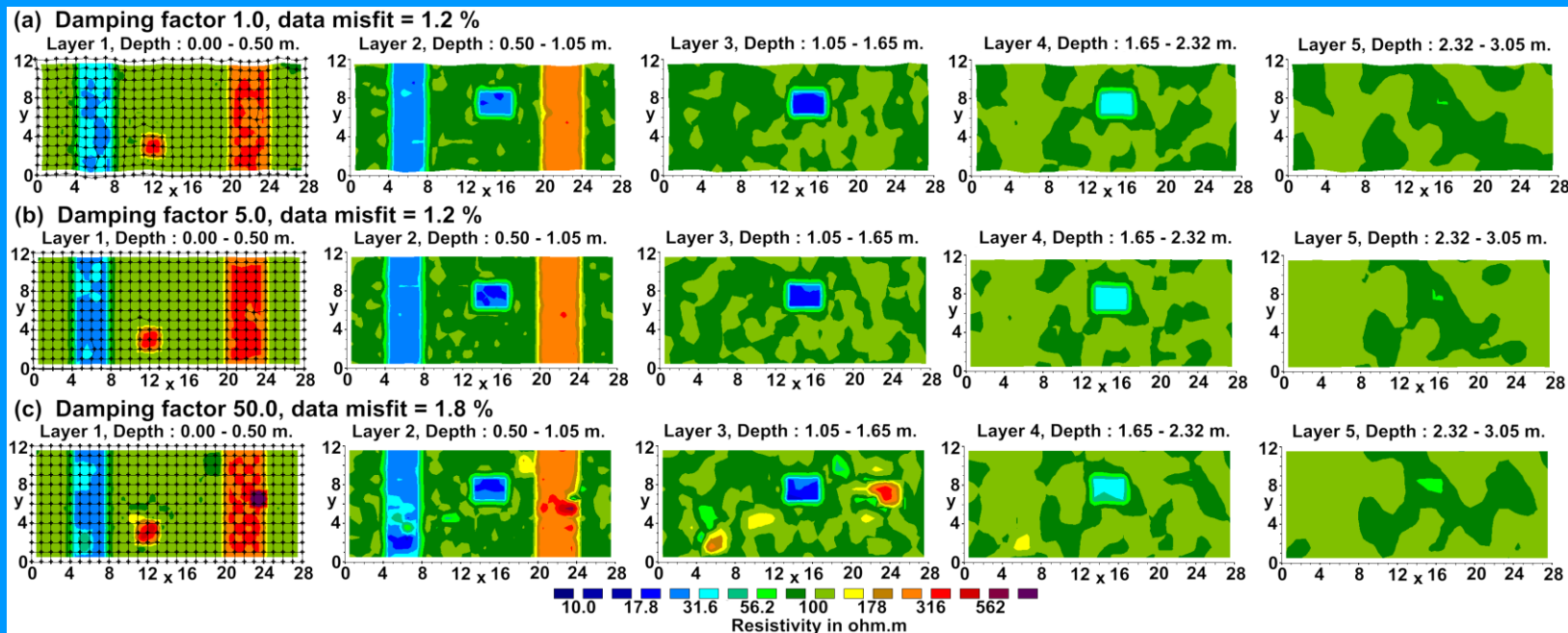
## 3-D test model – inversion with fixed electrodes

(a) The inversion model for the base data set matches the true structure with a data misfit of 1.2% (1.1% noise added). (b) The perturbed data set model shows significant distortions at the positions of the 4 shifted electrodes and a higher 1.8% data misfit. The 3 electrodes shifted horizontally show high-low resistivity anomaly pairs. The position of the electrode shifted upwards has a low resistivity anomaly. The inversion routine attempts to model the change in the potentials due to shifts in the electrodes by resistivity changes. A homogenous half space is used as the starting model.



# 3-D test model – inversion with shifting electrodes

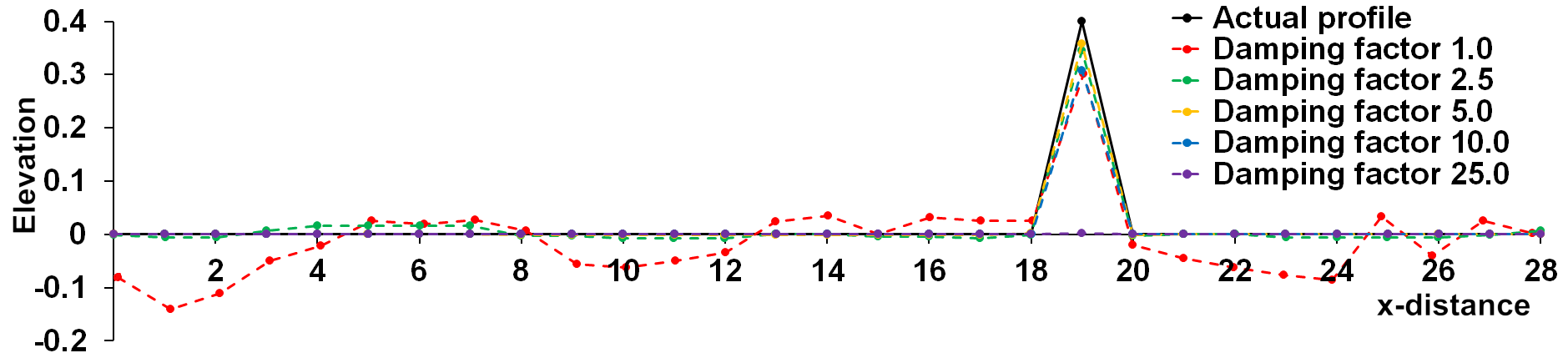
The artefacts are removed when the electrodes are allowed to shift during the inversion (a,b). The electrodes grid shows distortions with a damping factor of 1.0. It is expanded outwards over the low resistivity band and compressed inwards over the high resistivity band. The distortions in both the resistivity model and electrode positions are greatly reduced with a damping factor of 5.0.



### 3-D test model – profile plot

Figure below shows the  $x$ - $z$  surface profile along the  $y=10$  m line that crosses electrode 4 that was shifted upwards. The profile with a relative damping factor of 1.0 shows significant distortions that is greatly reduced when it is increased to 2.5, and largely eliminated with a value of 5.0. Using a damping factor greater than 5 reduces the upwards shift in the electrode position at the 19 m mark from the inversion compared to the actual shift.

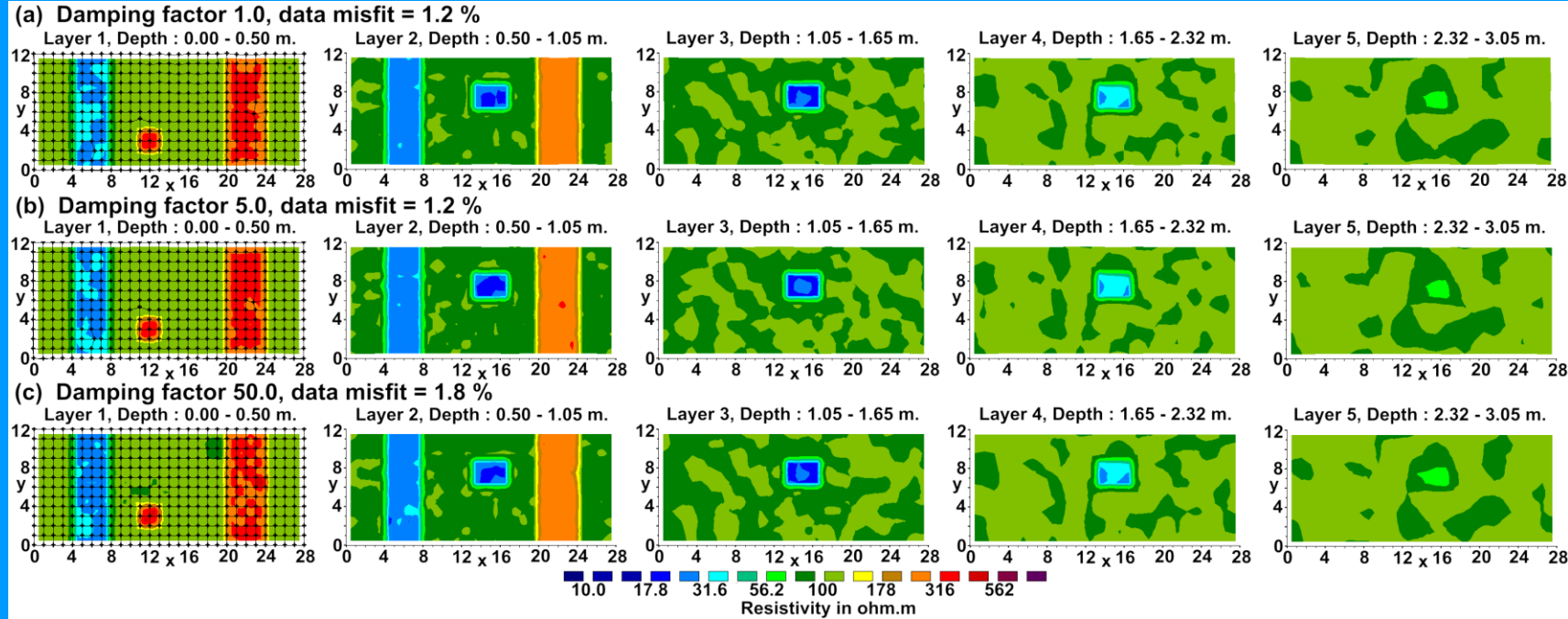
(a) Surface profile with homogenous half-space starting model





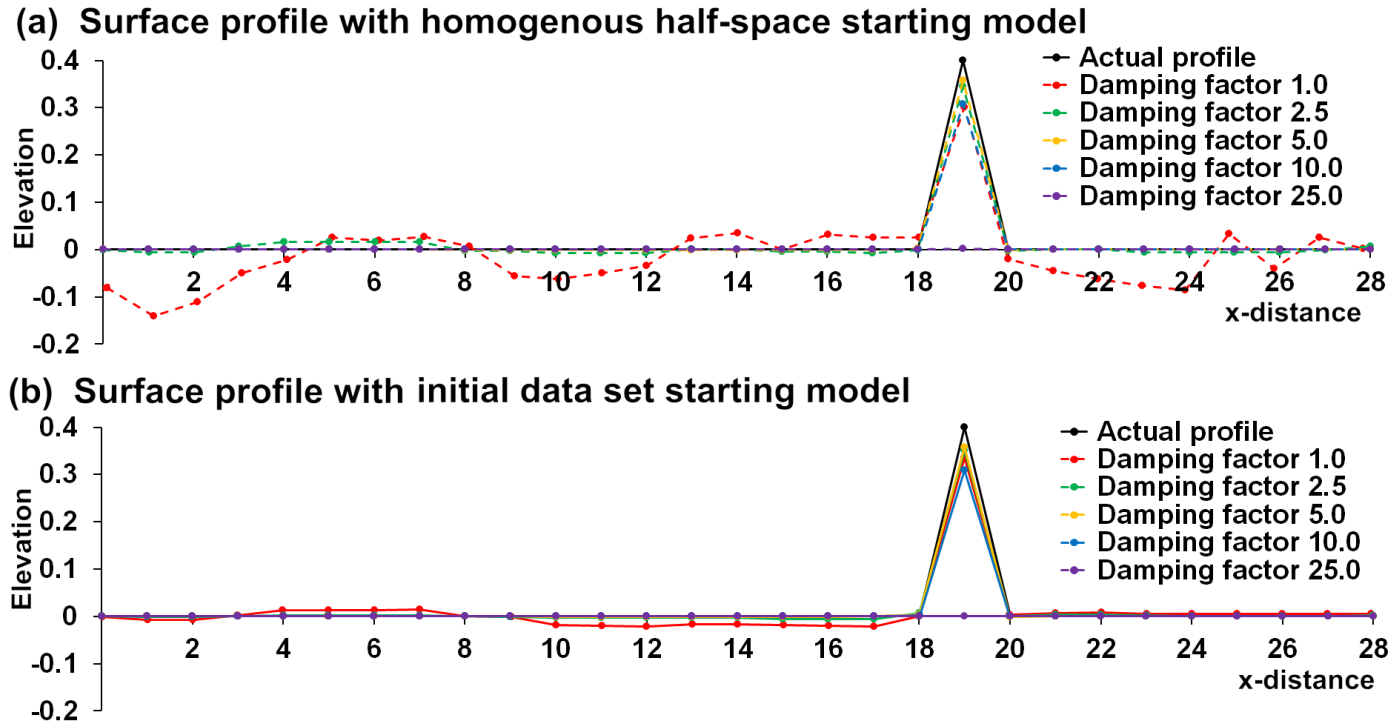
# 3-D test model – inversion with initial data set starting model

Figure shows the results obtained when the inversion model obtained for the initial data set is used as the starting model for the inversion of the perturbed data set. The distortions with damping factor of 1.0 are greatly reduced (a) and eliminated with a damping value of 5.0 (b). Using the model for the initial data set essentially carries out the inversion using the change in the apparent resistivity values.



### 3-D test model – profiles comparison

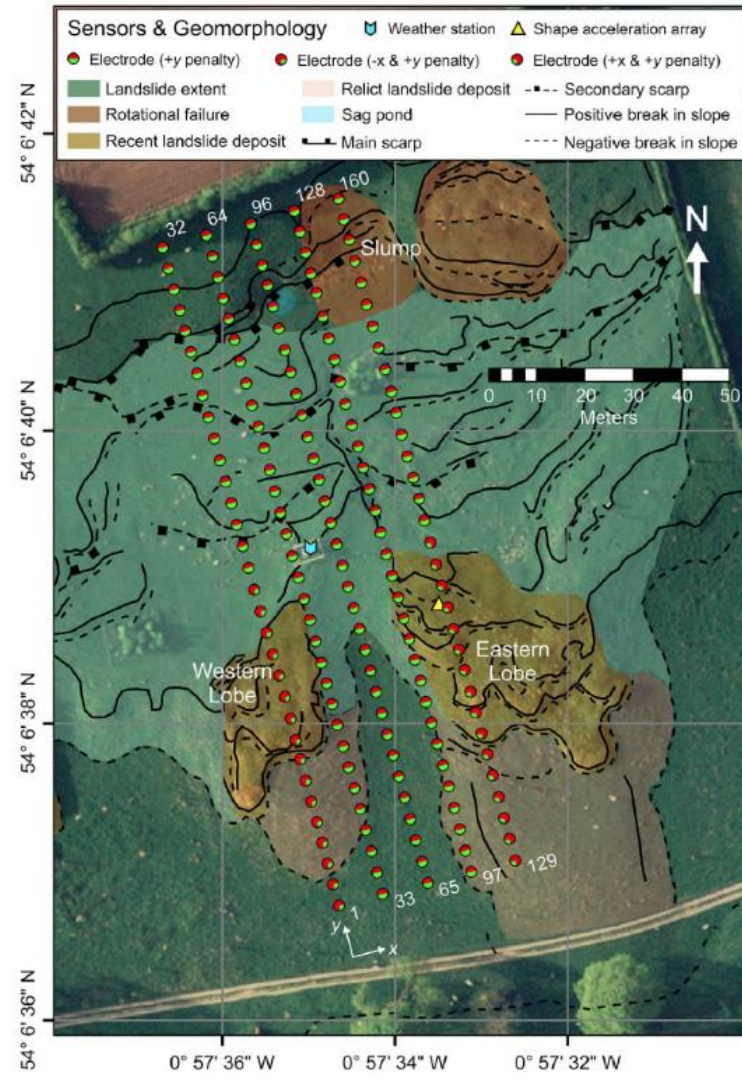
The profiles show the reduction in the distortions in the electrodes positions using the initial data set model as the starting model for the inversion of the perturbed data set more clearly. It is greatly reduced for a relative damping factor of 1.0 and almost completely eliminated with a value of 2.5.



## 3-D field data set

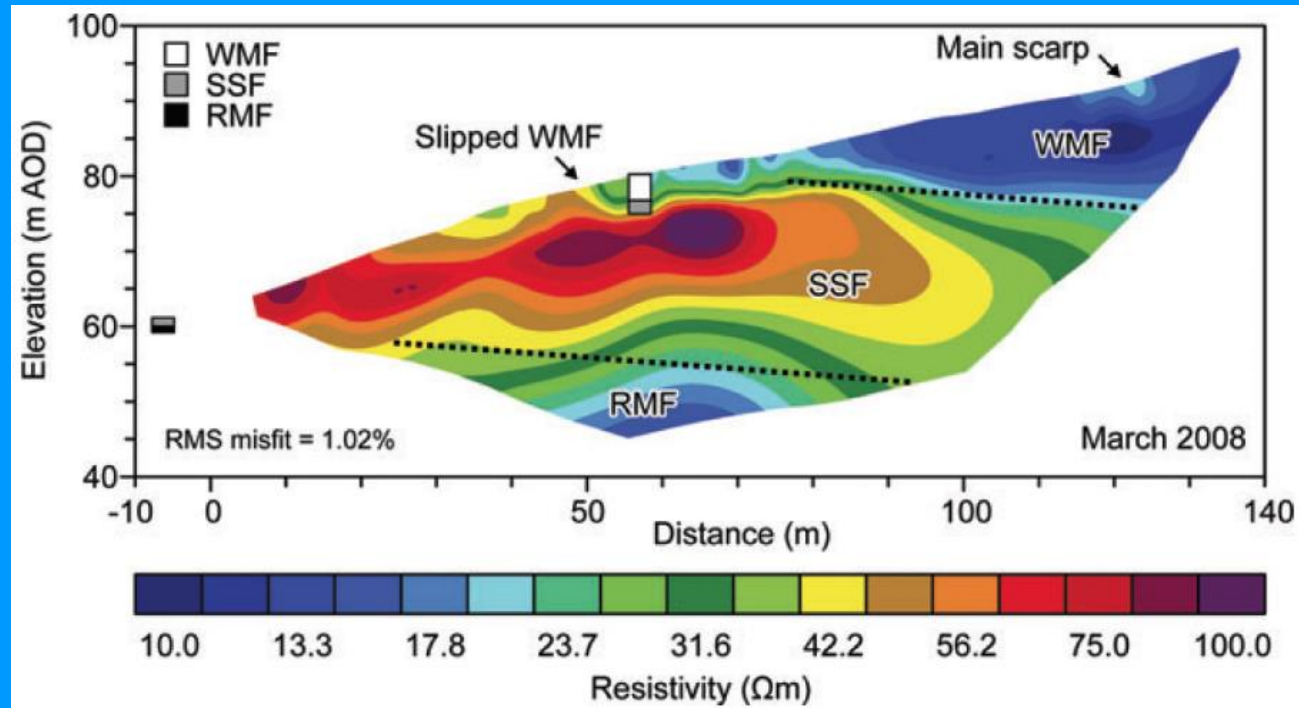
The survey site is on Hollin Hill near Malton U.K. which has a mean slope of  $14^\circ$ . Slope failure occurs at a mudstone formation in the upper part of the slope. The electrodes were initially laid out along 5 lines each with 32 electrodes with an inline spacing of 5 m and 10 m between the lines. Measurements were made using the inline dipole-dipole and cross-line equatorial dipole-dipole arrays.

An automatic geophysical monitoring system that can make daily measurements since March 2008 was used. Direct measurements of the electrodes positions were made much less frequently. Failure of the slope was observed to occur occasionally.



## Hollin Hill – geology

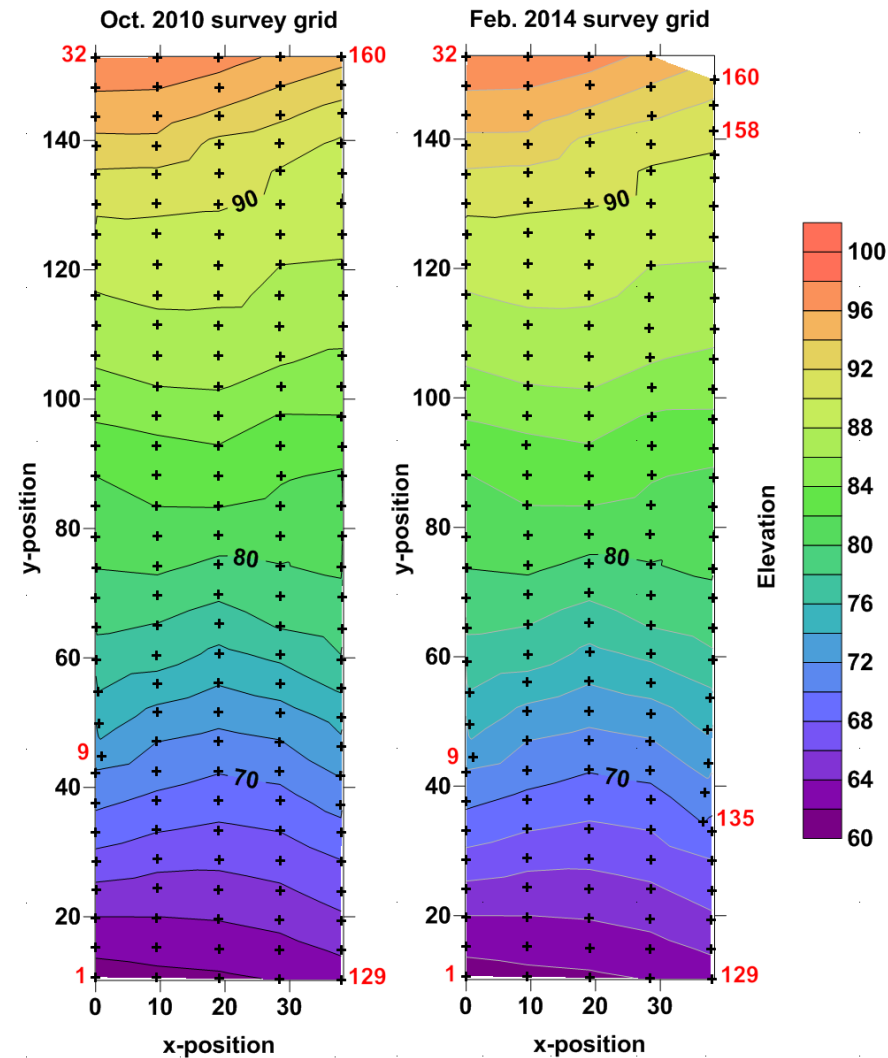
The results from a 2-D survey along one of the lines is shown with the geology. The main formations are the Lias Group Redcar Mudstone Formation (RMF), Staithes Sandstone & Cleveland Ironstone Formation (SSF) and Whitby Mudstone Formation (WMF) which is the failing formation at the upper part of the slope.



## Hollin Hill – ground movement

While a rectangular grid was originally laid out, movement of the electrodes occurred over time. The measured position from Oct. 2010 showed some movement near electrode 9. Another survey from Feb. 2014 showed significant shifts at electrodes 157 to 160 (at the top of the slope) and 135 to 137, and slight movement near electrode 9.

There was no significant movement at the bottom four rows of electrodes.

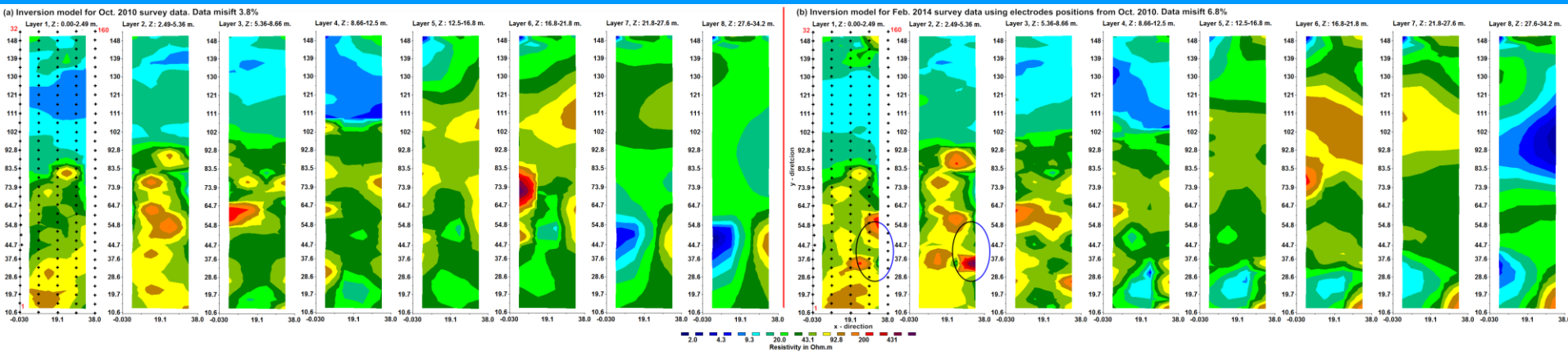




# Hollin Hill – inversion models with fixed electrodes

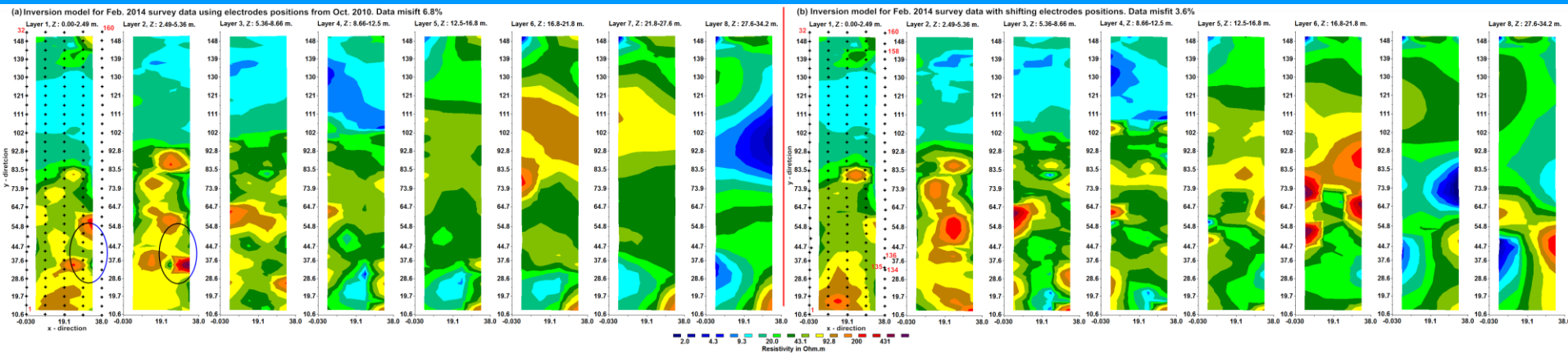
The inversion model from the survey carried out in Oct. 2010 is shown on the left in the form of layers starting from the top (a).

The right side shows the model for the data from the Feb. 2014 survey using the electrode positions measured in 2010. Since this does not take into account movement of the electrodes during that period, there are significant false resistivity anomalies particularly at the lower right side of the top two layers in the 2014 model (b).



# Hollin Hill – model with shifting electrodes

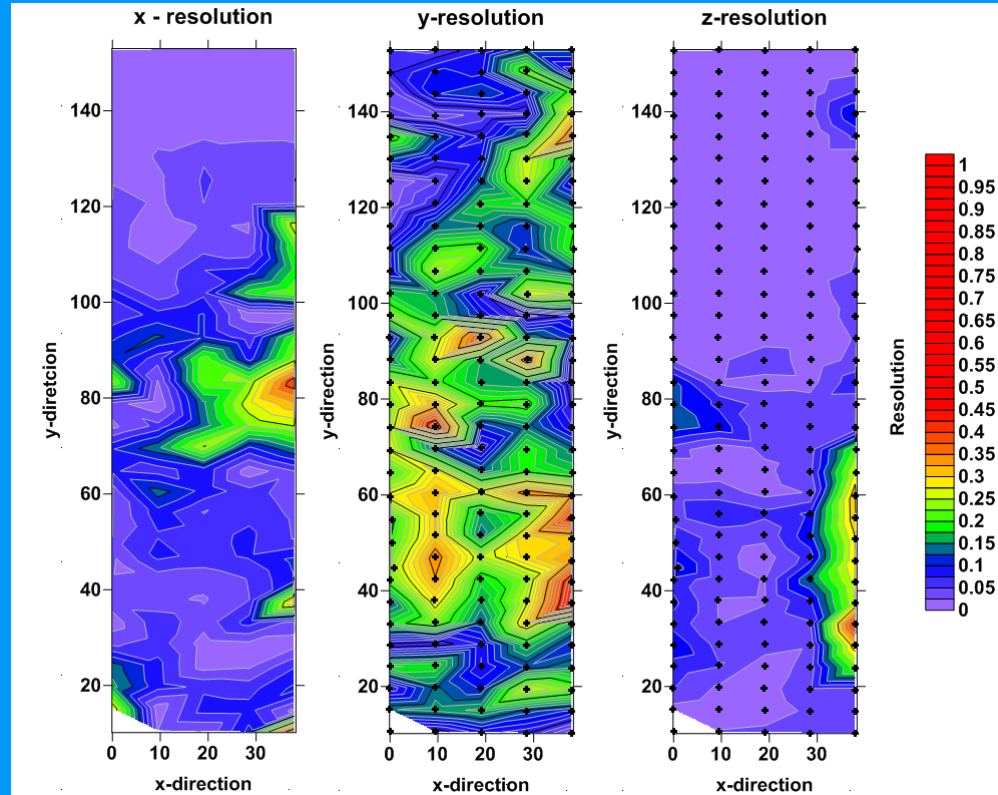
The inversion model where the electrodes are allowed to shift (b, right side) eliminates the resistivity artefacts between electrodes 136 to 138 compared to the model with fixed electrodes (a, left side). It also shows the downslope shift at electrodes 158 to 160. The amount of shifts in the model were 1.6, 1.8 and 1.1 m compared to the true values of 2.0, 3.2 and 3.8 m. The significantly smaller model shifts is probably because the electrodes are located near the top-right corner of the grid where there is less data. Furthermore it was found that the data from these electrodes was generally noisier than at other electrodes.



## Hollin Hill – electrodes movement resolution plots

Model resolution plots are commonly used to estimate the reliability of the model resistivity values. The resolution values vary from 0.0 (no resolution) to 1.0 (perfect resolution). The electrode positions resolution plots illustrate the degree

to which we can estimate the movement of the electrodes in different directions from the data set. The values depend on the set of arrays used and the model resistivity. As the inline dipole-dipole arrays that constitute most of the data points are aligned in the y-direction, the y-resolution plot has the highest values. The z-resolution plot generally has the lowest values showing that vertical electrode shifts are poorly detected.





# Conclusions

1. The least-squares inversion method can be modified to include the positions of the electrodes as model parameters.
2. The Jacobian matrix calculation time can be greatly reduced by using the adjoint-equation method.
3. The accuracy of the recovered electrode positions can be greatly improved by using the inversion model from an initial data set (with accurately measured electrode positions) as the starting model for the inversion of a later time data set. This eliminates the effect of the common background resistivity variations.
4. Selection of arrays used in the survey should also take into account the sensitivity to electrode movements so that they can be more accurately estimated from the apparent resistivity data.